X-RAY DIFFRACTION AND THERMAL ANALYSIS OF BAUXITE ORE-PROCESSING WASTE (RED MUD) EXCHANGED WITH ARSENATE AND PHOSPHATE

Paola Castaldi[1],*, Margherita Silvetti[1], Stefano Enzo[2], and Salvatore Deiana[1]

[1] Dipartimento di Scienze Ambientali Agrarie e Biotecnologie Agro-Alimentari, Sez. Chimica Agraria ed Ambientale, University of Sassari, Viale Italia 39, 07100 Sassari, Italy
[2] Dipartimento di Chimica, University of Sassari, Via Vienna 2, 07100 Sassari, Italy

Abstract—The use of waste materials from mineral ore processing has much potential for immobilizing pollutants such as arsenic (As) in natural soils and waters. The purpose of the present study was to investigate red mud (RM, a finely textured bauxite-ore residue) as a sequestering agent for arsenate and phosphate, including characterization of the types of surface complexes formed. The mineralogical and structural changes occurring in RM were investigated after exchange with arsenate [As(V)-RM] and phosphate [P(V)-RM] anions at pH 4.0, 7.0, and 10.0. Eight different phases were present in the untreated red mud (RM$_{nt}$), though 80 wt.% of the crystalline phase consisted of sodalite, hematite, gibbsite, and boehmite. The X-ray diffraction (XRD) data for As(V)-RM revealed an anion-promoted dissolution of the gibbsite, suggesting that this phase was the most active for As(V) sequestration. In addition, the lattice parameters of cancrinite were different in As(V)-RM at pH 7.0 and 10.0 from those in RM$_{nt}$. The changes may be related to the incorporation of arsenate in the cancrinite cages. X-ray diffraction patterns of P(V)-RM at pH 4.0 and 7.0 revealed the dissolution of sodalite, hematite, and gibbsite, and the formation of a novel phase, berlinite [(α,β)AlPO$_4$]. The new phases detected through XRD and thermal (TG/DTG) analysis in P(V)-RM probably originated through an initial phosphate-promoted dissolution of some RM phases, followed by a precipitation reaction between the phosphate and Al/Fe ions. The results obtained suggest that phosphate and arsenate, though with different reactivities, were strongly bound to some RM phases, such as gibbsite, cancrinite, sodalite, and hematite through mechanisms such as chemical sorption and coprecipitation reactions. The knowledge acquired will be helpful in selecting alternative materials such as red muds, which currently pose critical economic and environmental challenges related to their disposal, for the decontamination of soils and waters polluted with As.

Key Words—Arsenate, Phosphate, Red Muds, Thermal Analysis, XRD Diffraction.

INTRODUCTION

Arsenic (As) is a highly toxic and carcinogenic element which, under aerobic conditions, exists mainly in the form of oxyanion arsenate [AsO$_4^{3-}$] (Ruixia *et al.*, 2002; Wang and Mulligan, 2008). Concentrations of As in the environment can be substantially greater than background concentrations due to natural or anthropogenic factors or both, *e.g.* mining and smelting of metal sulfide ores, excessive or inappropriate use of pesticides and fertilizers containing arsenic, or weathering of As-bearing rocks (especially arsenopyrite) (Genç-Fuhrman *et al.*, 2005). A fraction of the total As concentration in soil can be soluble and leach to groundwater or become bioavailable to plants, microorganisms, and animals. The mobility in soil-pore water and the affinity of arsenate toward soil colloids needs to be better understood in order to evaluate appropriately the environmental impact of As. Many chemical and physical factors can affect both the sorption phenomena and the mobility of arsenate in soils and polluted waters:

pH, redox potential, the presence of oxides and oxyhydroxides of Fe and Al with complexing activity, the presence of organic matter with low and high molecular weight, and inorganic ions (Zhang and Selim, 2008). Other oxyacids commonly occurring in groundwater, such as H$_4$SiO$_4$, HCO$_3^-$, HSO$_4^-$, H$_2$PO$_4^-$, and HPO$_4^{2-}$, compete with arsenate for the same sorption sites on soil colloid surfaces (Ciardelli *et al.*, 2008) and are of particular importance. The affinity of arsenate and phosphate for Fe and Al oxyhydroxide surfaces, in particular, is similar (Manning and Goldberg, 1996; Antelo *et al.*, 2005). Indeed, P and As are both Group 5A elements and form chemical species with similar properties (Antelo *et al.*, 2005).

During the last ten years, in order to decrease the arsenate and phosphate concentrations in polluted waters, considerable attention has been paid to the use of different types of low-cost sorbents such as activated alumina (Ruixia *et al.*, 2002), Fe/Al/Mn oxides and hydroxides (Goldberg and Johnston, 2001; Luengo *et al.*, 2007; Luxton *et al.*, 2008), and red muds (Genç-Fuhrman *et al.*, 2005; Zhao *et al.*, 2009; Castaldi *et al.*, 2010a, 2010b).

Red muds (RM, finely textured residues derived from the digestion of bauxite during the Bayer process) are promising as sorbents for anions and cations (*e.g.* Garau *et al.*, 2007;

Huang *et al.*, 2008; Castaldi *et al.*, 2009, 2010a, 2010b; Zhao *et al.*, 2009), and their use for this purpose could provide an alternative to their mere disposal and, thus, lessen their negative environmental impact. Untreated and modified RM from different parts of the world have proven to be very efficient at blocking various pollutants such as heavy-metal cations (Castaldi *et al.*, 2008; Wang *et al.*, 2008; Smiljanić *et al.*, 2010), fluoride (Tor *et al.*, 2009), boron (Cengeloglu *et al.*, 2007), arsenate (Zhang *et al.*, 2008; Castaldi *et al.*, 2010a), phosphate (Zhao *et al.*, 2009; Castaldi *et al.*, 2010b), phenols (Tor *et al.*, 2009), *etc.* present in polluted waters. In laboratory and field studies, RM was effective at reducing the mobility of heavy metals (Gray *et al.*, 2006; Garau *et al.*, 2007) and arsenate and arsenite in contaminated soils (Lombi *et al.*, 2004; Garau *et al.*, 2011).

The composition of RM is generally complex because of the presence of several mineralogical phases, such as tectosilicate-like compounds and oxides and oxyhydroxides of Fe, Al, Ca, Si, and Ti (Zhao *et al.*, 2009; Castaldi *et al.*, 2008, 2010a). Such variability in composition influences the blocking properties of RM and their interaction mechanisms with anions. For such heterogeneous materials, identification of the more active phases involved in the adsorption reactions is important in order to determine the mode of anion bonding on the RM surfaces, and to identify the new chemical phases possibly formed after arsenate and phosphate sorption. However, recognizing and evaluating the structural changes occurring in RM after exchange with anions is a challenging task.

The objective of the present study was to evaluate, through X-ray diffraction (XRD) and thermal analysis (TA), the mineralogical and structural changes of RM exchanged separately with arsenate and phosphate at pH 4.0, 7.0, and 10.0. The pH values were chosen to cover the pH range generally found in soils and waters. The changes in RM saturated with arsenate and phosphate were compared because these anions have very similar acid dissociation constants of the protonated species, and are widely considered to have analogous adsorption characteristics (Zhang and Selim, 2008; Violante *et al.*, 2009). Phosphate can also be particularly effective in competing with As(V) for sorption sites on Al/Fe (oxyhydr)oxide mineral surfaces and this competition has the potential of influencing As mobility and bioavailability in the soil/water environment (Violante *et al.*, 2009). The experimental data were compared with those of untreated RM at the same pH values, in order to evaluate better the different reactivity and adsorbent properties of RM for the two anions.

MATERIALS AND METHODS

Characterization of the red muds

Red mud was obtained from the Eurallumina (Rusal group) refining plant in Portovesme, SW Sardinia, Italy.

The Bayer process is used there to refine bauxite from the Darling Ranges (Western Australia). Fresh red-mud (RM) samples, separated from the alumina through settling and filtration, were collected before the RM was discharged into an impound. In the laboratory, the RM samples were homogenized thoroughly and sub-samples were oven dried at 105ºC for 1 week in order to eliminate humidity and weakly bound adsorbed water (at this temperature, possible changes in the RM mineralogy and reactivity are avoided), finely ground and sieved to <0.02 mm (RM_{nt}). The characterization of RM_{nt} was described by Castaldi *et al.* (2008, 2010a). Briefly, the pH and electrical conductivity (EC) values were determined in distilled water (RM/slurries ratio of 1:2.5) using an Orion pH meter Model 420 A (C91-025CE Rau 13 probe) and an Analytical Model 131 Conductivity meter (01 2001 probe) (Table 1). The specific surface area of the RM_{nt} was determined by applying the BET model (S_{BET}) to the N_2 adsorption results obtained from a Carlo Erba Sorptomatic (Milan, Italy). The samples were pre-treated by outgassing at 40ºC combined with vacuum at 10^{-9} bar for 12 h. The error in determination of S_{BET} was ±3 m^2 g^{-1}. The total organic matter in the RM_{nt} was determined using the method of Walkley and Black described in the paper of Garau *et al.* (2007). The pH_{PZC} of RM_{nt} samples was measured by Laser Doppler Velocimetry coupled with Photon Correlation Spectrometry using a Coulter Delsa 440 spectrometer equipped with a 5 mW He-Ne laser (632.8 nm) (Castaldi *et al.*, 2008).

The total concentration of selected heavy metals in RM_{nt} samples was determined by drying the RM overnight at 105ºC and digesting it with a mixture of nitric acid and hydrochloric acid (HNO_3/HCl, 1:3 ratio), in a microwave Milestone MLS 1200. The heavy-metal concentrations were determined using a Perkin Elmer Analyst 600 flame atomic absorption spectrometer (FAAS) equipped with a HGA graphite furnace (Table 1).

The element composition was analyzed by means of Energy Dispersive X-ray (EDX) using a JEOL model JSM-6480LV (Table 1).

Anionic exchange

Adsorption studies were carried out in triplicate batches. All chemicals used were of reagent grade and were used without additional purification. Three batch experiments were prepared at pH 4.0, 7.0, and 10.0 and at constant temperature (25±1ºC). The RM samples (1.0 g each) kept at pH 4.0, 7.0, and 10.0 were doped separately with 25 mL of 0.4 M $Na_2HAsO_4·7H_2O$ and $Na_2HPO_4·7H_2O$ anionic solutions. The pH values of the RM and of the mixtures of RM/polluting solution were adjusted with HCl solutions, the concentrations of which were 0.01, 0.1, and 1.0 M, to keep the pH of the RM samples at 10.0, 7.0, and 4.0, respectively. The sorbent/anionic solutions were shaken for 24 h and 200 rpm at

Table 1. Properties of the RM_{nt} and RM samples at pH 10.0, 7.0, and 4.0 used in the study.

Chemical parameters	RM_{nt}	RM pH 10.0	RM pH 7.0	RM pH 4.0
pH	11.10 ± 0.12^d	10.0 ± 0.11^c	7.0 ± 0.13^b	4.0 ± 0.15^a
EC (mS·cm^{-1})	8.70 ± 0.14^c	8.25 ± 0.13^c	6.55 ± 0.15^b	5.22 ± 0.09^a
S_{BET}	19^a	21^{ab}	23^{bc}	25^c
PZC	4.77 ± 0.14	–	–	–
Organic matter (% d.m.)	0.60 ± 0.07	–	–	–
Pb (mg kg^{-1})	48.50 ± 5.6	–	–	–
Cd (mg kg^{-1})	1.46 ± 0.08	–	–	–
Cu (mg kg^{-1})	5.70 ± 0.23	–	–	–
Cr (mg kg^{-1})	640.21 ± 13.1	–	–	–
Element composition (wt.%)				
C	9.15 ± 0.24^a	9.0 ± 0.20^a	9.32 ± 0.18^a	n.d.
O	35.12 ± 1.36^a	34.23 ± 1.44^a	34.15 ± 1.56^a	42.33 ± 2.28^b
Na	5.17 ± 0.14^d	4.31 ± 0.13^c	2.30 ± 0.08^b	1.15 ± 0.11^a
Al	9.65 ± 0.58^a	10.25 ± 0.44^a	10.44 ± 0.72^a	9.33 ± 0.43^a
Si	4.32 ± 0.13^b	4.94 ± 0.11^b	4.53 ± 0.08^b	3.41 ± 0.09^a
Ca	1.04 ± 0.08^a	1.13 ± 0.08^a	1.15 ± 0.07^a	1.00 ± 0.09^a
Fe	30.35 ± 2.6^a	30.88 ± 2.2^a	32.53 ± 3.2^a	35.32 ± 3.6^b
Ti	4.13 ± 0.12^a	4.23 ± 0.09^a	4.53 ± 0.07^a	6.43 ± 0.08^b
Cl	1.07 ± 0.03^a	1.03 ± 0.04^a	1.05 ± 0.03^a	1.03 ± 0.03^a

* Mean values±standard deviations followed by the same letter within a row do not differ significantly (Fisher's LSD test, $P<0.05$).

25ºC, which was proved beforehand to be sufficient for reaching equilibrium. Two other identical treatments with the anionic solutions were carried out on the same RM samples. After the anion-exchange process, the RM samples were washed with 25 mL of distilled water.

After each step, the solid and liquid phases were separated by centrifugation at 10,000 rpm for 20 min and the supernatant filtered through a 0.20 µm pore size, cellulose membrane filter. The samples obtained were air dried for 5−6 days. The total concentration of arsenate and phosphate sorbed by the RM samples was determined by drying the respective RM samples overnight at 105ºC and digesting them with HNO_3 and HCl (ratio 1/3) in a Milestone MLS 1200 microwave. The As(V) and P(V) were measured by ion chromatography using a Dionex LC 20 equipped with an IonPac AS12A 4 mm Analytical Column and an IonPac AG12A Guard Column. Carbonate 1.8 mM/bicarbonate 1.7 mM was employed as the eluent at a flow rate of 1.5 mL/min. The sample loop volume was 10 µL.

Powder XRD analysis

X-ray diffraction analysis was carried out on RM_{nt} (Castaldi *et al.*, 2008, 2010a), on unexchanged RM, and on RM exchanged separately with arsenate and phosphate at pH 4.0, 7.0, and 10.0.

The XRD analysis was carried out using a Rigaku D/MAX diffractometer (CuKα). The X-ray generator worked at 40 kV and 40 mA, the goniometer was equipped with a diffracted-beam graphite monochromator, the patterns were collected in the angular range from 10 to 100º2θ with a 0.05º2θ step size. Before analysis, RM_{nt}, unexchanged RM, and RM exchanged with arsenate and phosphate at pH 4.0, 7.0, and 10.0 were dried at 65ºC for 8 h. After that, samples were dried at 140ºC for 8 h to eliminate humidity and weakly bound adsorbed water; then the XRD patterns of all the samples were recorded. The data collection was performed overnight (~12 h per pattern). For a 2θ-scan of 90º with a step-size of 0.05º2θ, this is equivalent to ~24 s per point.

Crystalline phases were identified with a search-match procedure using the database of the International Center for Diffraction Data for Inorganic Substances (Inorganic Crystal Structure Database) (Budroni *et al.*, 2000) (Table 2). Aside from crystalline phases, ~20% of the RM consisted of amorphous oxides. The powder patterns were then analyzed quantitatively according to the Rietveld method (Young, 1993). The estimated standard error of the phases was supplied by the procedure, based on the assumption of a uniform and normal distribution of residuals. The technique is sensitive to the crystalline phase contents listed above of 1−2 wt.%, and the estimated standard error may be as large as 3−4 wt.% for the more abundant phases. This level of sensitivity is not ascribed to the numerical Rietveld method but mainly to the diffraction-pattern collection strategy.

Thermal analysis

Thermogravimetry (TG) and differential thermogravimetry (DTG) of unexchanged RM and of RM

Table 2. Chemical phases of the RM_{nt} and RM samples unexchanged and exchanged with arsenate and phosphate at pH 10.0, 7.0, and 4.0 (wt.%) (140°C)*.

	RM pH 11.1 RM_{nt}	RM-10	RM pH 10.0 As(V)-RM	P(V)-RM	RM-7	RM pH 7.0 As(V)-RM	P(V)-RM	RM-4	RM pH 4.0 RM-As(V)	P(V)-RM
Cancrinite [$Na_6Ca_{1.5}Al_6Si_6O_{24}(CO_3)_{1.6}$]	4.0 ± 0.5^a	4.0 ± 0.5^a	11.0 ± 0.5^c	n.d.	3.5 ± 0.5^a	6.0 ± 0.5^b	n.d.	n.d.	n.d.	n.d.
Sodalite [$Na_8(Cl,OH)_2|Al_6Si_6O_{24}$]	20.0 ± 2.0^a	24.0 ± 2.0^{ab}	26.0 ± 2.5^b	25.0 ± 2.0^b	24.0 ± 2.0^{ab}	26.0 ± 2.5^b	n.d.	22.0 ± 2.0^a	21.0 ± 2.0^a	n.d.
Hematite [Fe_2O_3]	44.0 ± 3.0^b	42.0 ± 3.0^b	41.0 ± 3.0^{ab}	50.0 ± 3.0^c	42.0 ± 3.0^b	43.0 ± 3.0^b	53.0 ± 3.0^c	49.0 ± 3.0^c	51.0 ± 3.0^c	39.0 ± 3.0^a
Boehmite [AlO(OH)]	12.0 ± 2.0^{ab}	12.0 ± 2.0^{ab}	8.0 ± 2.0^a	11.0 ± 2.0^{ab}	12.0 ± 2.0^{ab}	10.0 ± 2.0^{ab}	18.0 ± 2.0^c	8.0 ± 2.0^a	13.0 ± 2.0^b	20.0 ± 2.0^c
Gibbsite [$Al(OH)_3$]	4.0 ± 0.5^a	4.0 ± 0.5^a	n.d.	3.0 ± 0.5^a	4.0 ± 0.5^a	n.d.	n.d.	4.0 ± 0.5^a	n.d.	n.d.
Anatase [TiO_2]	4.5 ± 0.5^a	4.0 ± 0.5^a	4.0 ± 0.5^a	5.0 ± 0.5^{ab}	4.0 ± 0.5^a	4.0 ± 0.5^a	7.0 ± 0.5^c	5.5 ± 0.5^b	4.5 ± 0.5^a	9.0 ± 0.5^d
Andradite [Ca-Fe-Al-Si oxide]	5.5 ± 0.5^b	5.0 ± 0.5^{ab}	5.0 ± 0.5^{ab}	4.0 ± 0.5^a	5.0 ± 0.5^{ab}	5.0 ± 0.5^{ab}	6.0 ± 0.5^b	5.5 ± 0.5^b	5.5 ± 0.5^b	8.0 ± 0.5^c
Quartz [SiO_2]	6.0 ± 0.5^b	5.0 ± 0.5^b	5.0 ± 0.5^b	2.0 ± 0.5^a	5.5 ± 0.5^b	6.0 ± 0.5^b	9.0 ± 0.5^c	6.0 ± 0.5^b	5.0 ± 0.5^b	11.0 ± 0.5^c
Berlinite [$(\alpha, \beta)AlPO_4$]	n.d.	n.d.	n.d.	n.d.	n.d.	n.d.	7.0 ± 1.5^a	n.d.	n.d.	13.0 ± 2.5^b

* Mean values±standard deviations followed by the same letter within a row do not differ significantly (Fisher's LSD test, $P<0.05$).

exchanged with arsenate and phosphate at pH 4.0, 7.0, and 10.0 were performed using a Netzsch STA 429 thermal analysis apparatus. The samples were heated in a platinum crucible in the temperature range $25-800°C$ with a heating rate of $10°C/min$ in air. The flow rate of the air was 10 mL/min. About 30 mg of the sample was used in each run. The water concentration in the samples was determined from the TG curve mass loss.

Statistical analysis

All of the data presented are the mean of three replicates. One-way analysis of variance (One-way ANOVA) was carried out to compare all the means from different treatments. Where significant P values ($P<0.05$) were obtained, differences between individual means were compared using the post-hoc Fisher's least significant difference test (LSD, $P<0.05$). All data were analyzed using the *NCSS* software (*Number Cruncher Statistical Systems*, Kaysville, Utah, USA (http://www.ncss.com/ncss.html) for Windows.

RESULTS AND DISCUSSION

Chemical, physical, and structural characteristics of red-mud samples

The properties of the RM samples at different pH values used in the study are reported in Table 1. The specific surface areas of RM at pH 4.0, 7.0, and 10.0 were 25, 23, and 21 m^2 g^{-1}, respectively (Table 1). The pH_{pzc} of the RM_{nt} samples was 4.77, which is significantly different from values found in the literature ($pH_{pzc} = 8-8.5$) (*e.g.* Pradhan *et al.*, 1999), probably due to the large aluminosilicate content of the present samples. Analyses by EDX revealed that the unexchanged RM was rich in O (35.12 wt.%), Fe (30.35 wt.%), Al (9.65 wt.%), and C (9.15 wt.%) (Table 1). A mixture of eight phases was retrieved in RM_{nt} samples, though note that 80 wt.% of the RM crystalline phase consisted of Fe and Al oxides and

oxyhydroxides such as hematite, boehmite, and gibbsite, and tectosilicates such as sodalite (Table 2). The XRD analysis showed that the different pH values changed the mineralogical composition of the red-mud samples. At pH 4.0 a proton-promoted loss of acid-soluble fractions such as boehmite and cancrinite was observed.

XRD analysis of red-mud samples exchanged with arsenate and phosphate

The maximum quantity of arsenate adsorbed on RM followed the order: As(V)-RM pH 4.0 (1.908 mmol g^{-1}) > As(V)-RM pH 7.0 (0.174 mmol g^{-1}) > As(V)-RM pH 10.0 (0.118 mmol g^{-1}) (Castaldi *et al.*, 2010a). The maximum quantity of phosphate adsorbed on RM was as follows: P(V)-RM pH 4.0 (4.871 mmol g^{-1}) > P-RM pH 7.0 (0.924 mmol g^{-1}) > P-RM pH 10.0 (0.266 mmol g^{-1}) (Castaldi *et al.*, 2010b). The quantities of phosphate and arsenate sorbed onto the same RM were very different, *e.g.* the phosphate sorbed onto RM at pH 4.0 was three times greater than arsenate at the same pH. Such a difference is out of line with a rather general literature consensus, which considers phosphate and arsenate as having similar adsorption behavior on solid surfaces (*e.g.* Antelo *et al.*, 2005). This apparent discrepancy could be explained by a different ligand-exchange mechanism for the two anions and/or by a difference in reactivity and precipitation behavior of phosphate compared with arsenate anions on the surfaces of RMs (Zhao *et al.*, 2009).

The mineralogical and structural changes which occurred in the RM samples following sorption of the arsenate and phosphate were determined by XRD and thermal analysis (Tables 2−4; Figures 1−4).

XRD analysis of As(V)-RM. The XRD analyses of As(V)-RM at pH 4.0, 7.0, and 10.0 indicated that the lattice parameters of some RM phases, such as hematite, boehmite, and sodalite, were largely unchanged with respect to unexchanged RM at the same pH values

Table 3. Lattice parameters of the main constituents of RM_{nt} and RM samples unexchanged and exchanged with arsenate and phosphate at pH 10.0, 7.0, and 4.0 (error associated with the unit-cell parameters ± 0.001)[*].

| | Cancrinite (SG $P6_3$) | | Sodalite (SG $P\bar{4}3n$) | Hematite (SG $R\bar{3}c$) | |
	a (Å)	c (Å)	a (Å)	a (Å)	c (Å)
RM_{nt}	12.724[b]	5.179[a]	8.993[a]	5.027[a]	13.748[a]
RM pH 4.0	—	—	8.979[a]	5.032[a]	13.761[a]
RM pH 7.0	12.717[b]	5.177[a]	8.992[a]	5.034[a]	13.748[a]
RM pH 10.0	12.782[b]	5.168[a]	8.972[a]	5.025[a]	13.727[a]
As(V)-RM pH 4.0	—	—	8.978[a]	5.027[a]	13.757[a]
As(V)-RM pH 7.0	12.302[a]	5.322[b]	8.977[a]	5.027[a]	13.746[a]
As(V)-RM pH 10.0	12.304[a]	5.318[b]	8.988[a]	5.032[a]	13.747[a]
P(V)-RM pH 4.0	—	—	—	5.023[a]	13.731[a]
P(V)-RM pH 7.0	—	—	—	5.019[a]	13.728[a]
P(V)-RM pH 10.0	—	—	9.008[a]	5.022[a]	13.742[a]

* Mean values followed by the same letter within a column do not differ significantly (Fisher's LSD test, $P<0.05$).

Table 4. Weight losses (percentage of total sample weight) corresponding to the main peaks shown in the thermograms and temperature ranges (ºC) in which they occur recorded by TG analysis on RM samples unexchanged and exchanged with arsenate and phosphate at pH 10.0, 7.0, and 4.0[*].

	25−200ºC	200−400ºC	400−600ºC	600−800ºC
RM pH 4.0	17.47±0.95[d]	2.90±0.37[ab]	1.95±0.10[b]	1.51±0.21[b]
RM pH 7.0	4.98±0.41[b]	4.19±0.53[c]	3.33±0.28[e]	2.06±0.27[c]
RM pH 10.0	3.95±0.57[a]	4.16±0.57[c]	2.95±0.21[d]	2.05±0.27[c]
As(V)-RM pH 4.0	11.18±0.96[c]	2.40±0.28[a]	1.54±0.11[a]	0.74±0.18[a]
As(V)-RM pH 7.0	3.97±0.66[a]	5.40±0.57[d]	2.92±0.27[d]	0.80±0.21[a]
As(V)-RM pH 10.0	3.08±0.55[a]	5.29±0.57[d]	2.47±0.11[c]	1.13±0.24[b]
P(V)-RM pH 10.0	3.61±0.35[a]	3.34±0.46[b]	2.95±0.29[d]	1.95±0.20[c]
	25−180ºC	180−260ºC	260−400ºC	400−800ºC
P(V)-RM pH 4.0	5.98±0.27[b]	2.70±0.15[a]	2.98±0.19[a]	2.88±0.34[b]
P(V)-RM pH 7.0	4.06±0.33[a]	3.49±0.31[b]	2.72±0.17[a]	1.73±0.15[a]

[*] Mean values±standard deviations followed by the same letter within a column do not differ significantly (Fisher's LSD test, $P<0.05$).

(Table 3). By contrast, significant changes in lattice parameters of the cancrinite phase were observed in As(V)-RM at pH 7.0 and 10.0 (Table 3). The cancrinite framework (hexagonal $P6_3$) consists of alternating Si−O−T units (T = Si or Al) derived from SiO_4 and AlO_4 tetrahedra (Mon *et al.*, 2005). The tetrahedral arrangement determines the formation of cages and channels typical of the open porous structure of zeolites (Mon *et al.*, 2005). The main wide channel can host cations and anions such as carbonate, nitrate, chromate, molybdate, and hydroxyl groups, whereas the small cages contain only cations and water molecules (Mon *et al.*, 2005). The cancrinite phase present in the RMs used in this study hosted carbonate and nitrate as non-structural anions, as previously highlighted by Fourier-transform infrared (FTIR) analyses (Castaldi *et al.*, 2008, 2010a). Comparison of the lattice parameters of cancrinite for the untreated and unexchanged RMs and
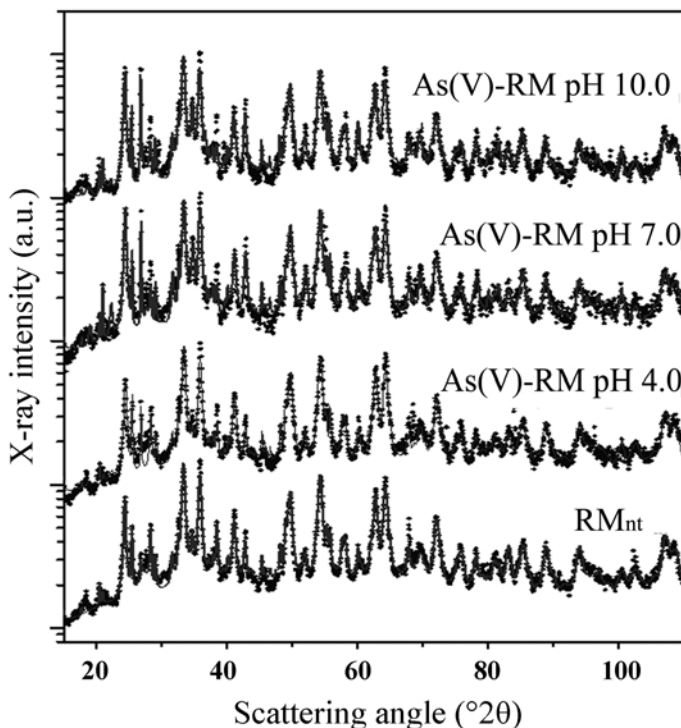

Figure 1. Data points of experimental XRD patterns and full lines after Rietveld refinement for the RMₙₜ and RM samples exchanged with arsenate at pH 4.0, 7.0, and 10.0. The close match between experiment and calculation testify to the accuracy of the structure description of the four red-mud systems.
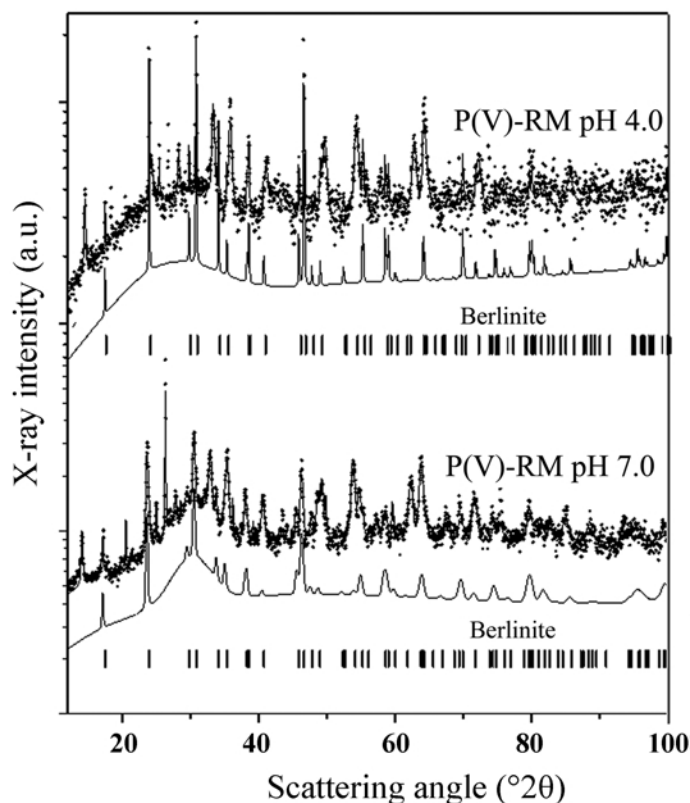
Figure 2. Data points for experimental XRD patterns and full lines after Rietveld refinement for the P(V)-RM at pH 4.0 and 7.0. The curve and the lines at the bottom are the contribution to the simulation of the P(V)-RM at pH 4.0 and 7.0 of the berlinite phase alone.

for RM doped with arsenate, revealed a decrease in 'axis *a*' and an increase in 'axis *c*' in As(V)-RM at pH 7.0 and 10.0, which narrows (1.73 Å average) the distribution of Si−O distances.. The changes could be assigned to an incorporation of arsenate anions in the cages of this aluminosilicate framework. Indeed, as the openings of cancrinite cages [5.90 Å; (Mon *et al.*, 2005)] are compatible with the size of arsenate anions [anionic radius of AsO_4^{3-} = 2.37 Å; (Rojsajjakul *et al.*, 1997)], the latter could have replaced the CO_3^{2-} anions [anionic radius of CO_3^{2-}: 1.71 Å; (Rojsajjakul *et al.*, 1997)] located in the cages of cancrinite in RMs at pH 7.0 and 10.0.

In all of the As(V)-RM samples, XRD analyses indicated a total 'ligand-promoted' dissolution of the gibbsite phase [$Al(OH)_3$] (Table 2). The dissolution could have caused the formation of Al arsenate, probably present as an amorphous precipitate on the RM surfaces, and, therefore, undetectable by XRD analyses. The XRD data showed that gibbsite was the more active phase for As(V) sorption. The gibbsite content in RM is generally small, however, and the significant adsorption of As(V) detected (*e.g.* 1.908 mmol g^{-1} in As(V)-RM pH 4.0) could be justified by the contribution of other phases, such as cancrinite and hematite.

XRD analysis of P(V)-RM

Analysis by XRD revealed that no appreciable changes occurred in the lattice parameters of some selected phases of unexchanged RM and phosphate-exchanged RM at different pH values (Table 3).

A total dissolution of gibbsite, sodalite, and cancrinite phases was observed in P(V)-RM at pH 4.0 and 7.0 (Table 2). This was exclusively phosphate-promoted at pH 7.0, while at pH 4.0 the whole effect could be due both to addition of phosphate and to chemical acidity (Table 2). A significant decrease in hematite was finally observed only in the P(V)-RM at pH 4.0 (Table 2). After the addition of phosphate to the RM at pH 4.0 and 7.0, 13 and 7 wt.%, respectively, of the new phase, berlinite, was observed in the XRD patterns (Figure 2). The new phase probably originated through phosphate precipitation processes with Al ions from the ligand-promoted dissolution of sodalite and gibbsite. By contrast, in P(V)-RM at pH 4.0, no precipitated Fe phosphate phase was found in the XRD analyses. The partial dissolution of the hematite phase could have caused the formation of amorphous Fe-phosphate precipitates undetectable by XRD (Scaccia *et al.*, 2002).

The results obtained by XRD analysis showed that the RMs used in the present study were capable of sequestering the arsenate and phosphate mainly through

precipitation reactions and sorption and substitution processes, and the phases involved in the sequestration of these anions were gibbsite, sodalite, cancrinite, and hematite.

Thermal analysis of RM samples

Thermal analysis (TG/DTG) of RM samples exchanged with arsenate and phosphate at pH 4.0, 7.0, and 10.0 were carried out and compared with the unexchanged RM at the same pH values. Similar stages of weight losses were detected in the unexchanged RM, As(V)-RM, and P(V)-RM samples (Table 4, Figures 3−4).
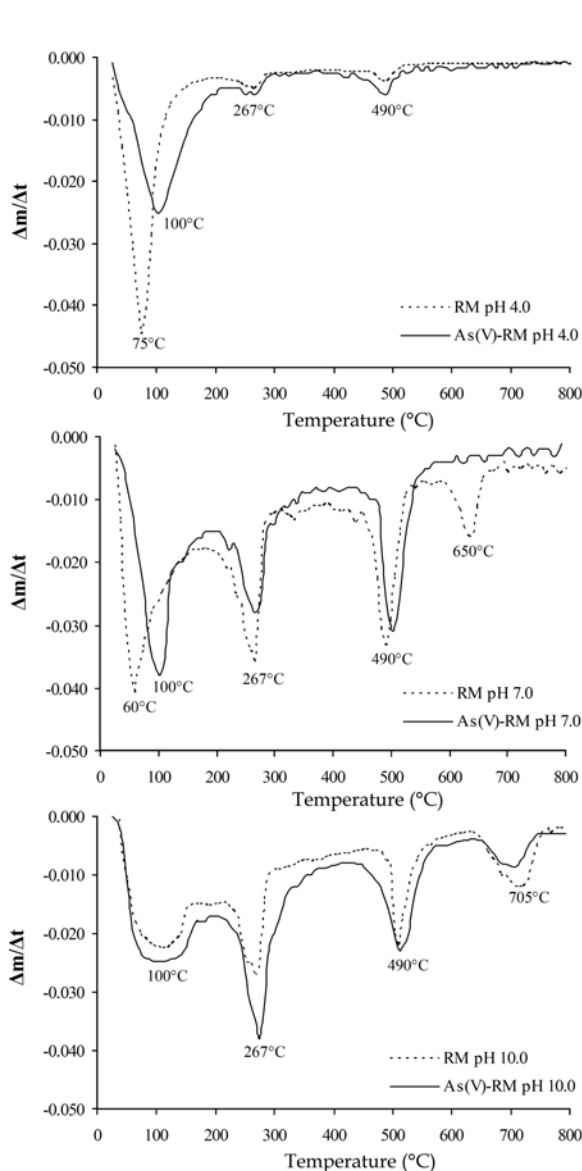
Thermal analysis of unexchanged RM samples at pH 4.0, 7.0, and 10.0. The DTG thermograms of unexchanged RM samples at different pH values showed a weight loss in the 25−200ºC temperature range, which can be attributed to the superficially adsorbed water, with peak temperatures varying depending on the RM sample (Figures 3−4). The weight losses in this range of temperature followed the order: RM pH 4.0 > RM pH 7.0 > RM pH 10.0; the trend could be due to the acidification of the sorbent (Table 4). The weight losses detected in the 200−400ºC range, with a peak at 267ºC, can be associated with the loss of water molecules located in the channels and cages of the cancrinite and

Figure 3. DTG graphs of RM unexchanged and exchanged with arsenate at pH 4.0, 7.0, and 10.0.
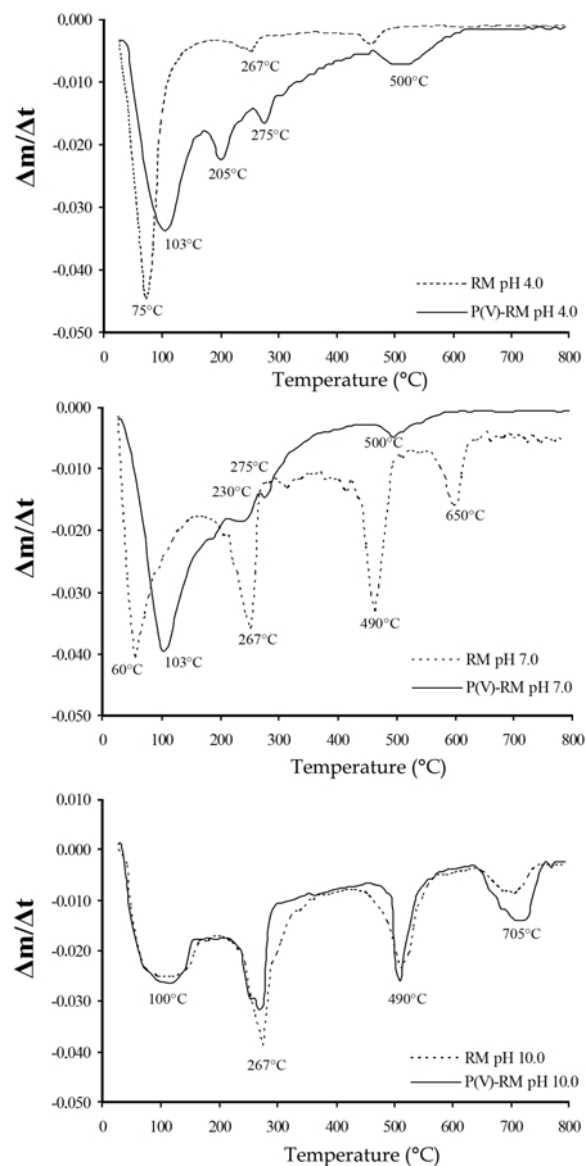
Figure 4. DTG graphs of RM unexchanged and exchanged with phosphate at pH 4.0, 7.0, and 10.0.

sodalite structures, and bound to the non-framework anions and cations present in both tectosilicates (Castaldi *et al.*, 2008). The reduced weight losses in this temperature range for the unexchanged RM samples at pH 4.0 could be due to a dissolution of cancrinite phase attributable to the acidification of the RM, as indicated by the XRD analyses, which showed the complete disappearance of this phase at pH 4.0 (Table 2).

The thermal events recorded in the range 400−600ºC, which showed a peak at 490ºC, can be ascribed to a synergistic effect of the release of CO_3^{2-} groups coming from cancrinite (Linares *et al.*, 2005), the decomposition of gibbsite (Pontikes *et al.*, 2007), and the dehydration of boehmite to form Al oxide phases (Sglavo *et al.*, 2000) (Figures 3−4). In the RM samples, at pH 4.0 the peak at 490ºC is markedly decreased in its intensity probably because the acid pre-treatment favored the dissolution of carbonates and bohemite (Castaldi *et al.*, 2008; Figures 3−4).

Finally, in the unexchanged RM at pH 7.0 and 10.0, another weight loss, in the 600−800ºC range, was observed (Figures 3−4). The weight loss may be attributed to the release of CO_2 during decomposition of calcite (Liu *et al.*, 2007). However, the calcite phase was not detected by XRD, probably because it was present at concentrations below the detection limit (<2 wt. %) or as an X-ray amorphous phase. The temperature of the peak corresponding to the release of CO_2 was at ~650ºC and 705ºC in RM at pH 7.0 and 10.0, respectively. This increase in temperature following the increase in pH suggests that more energy was needed for the thermal decomposition of calcite in the RM at pH 10.0, which was better crystallized than the calcite in the RM at pH 7.0.

Thermal analysis of As(V)-RM samples at pH 4.0, 7.0, and 10.0. The first weight loss (25−200ºC) in DTG thermograms of As(V)-RM, but also of P(V)-RM, at pH 4.0 and 7.0 shifted toward higher temperatures with respect to the same unexchanged RM, with a peak temperature of 100−103ºC (Figures 3−4). The increased thermal stability of this entity could be due to a stronger network of hydrogen bonds between the hydroxides of the different phases of RM and the hydrated arsenate and phosphate anions, as indicated by Palmer *et al.* (2009). A smaller weight loss in the RM samples exchanged with arsenate and phosphate at pH 4.0 and 7.0 with respect to unexchanged RM was observed (Table 4).

The weight losses recorded in the 200−400ºC range were greater in As(V)-RM at pH 7.0 and 10.0 compared to unexchanged RM at the same pH values (Table 4). This trend could be due to a greater loss of hydration molecules bound to non-framework anions located in the channels of the cancrinite structure of RM samples exchanged with arsenate at pH 7.0 and 10.0. This may be better explained with the hypothesis, supported by XRD,

which showed significant changes in the cancrinite lattice parameters, that a partial substitution of carbonate by arsenate anions occurred. Indeed, the possibility that each cation and/or anion must interact with the sorbent reactive sites depends on its charge density, which is a consequence of both the ion size and the total negative or positive charge. The CO_3^{2-} anion has an ionic radius (1.71 Å) less than that of the AsO_4^{3-} anion (2.37 Å) (Rojsajjakul *et al.*, 1997), though at pH 7.0 and 10.0 the anion carbonate exists mainly as a monovalent anion HCO_3^- ($pK_{a1} = 6.36$ and $pK_{a2} = 10.20$), while at the same pH values the divalent anion $HAsO_4^{2-}$ ($pK_{a1} = 2.3$; $pK_{a2} = 6.8$ and $pK_{a3} = 11.6$) dominates. Consequently, the greater weight losses recorded in the RM samples doped with arsenate at pH 7.0 and 10.0, with respect to unexchanged RM, could be due to the greater hydration sphere of arsenate anions which have a greater negative charge and, therefore, a greater polarizing power and larger capacities for bound water molecules.

The smaller weight losses in the range 400−600ºC in As(V)-RM at pH 4.0, 7.0, and 10.0, compared to unexchanged RM, could be due to arsenate-promoted solubilization of gibbsite (Table 4). The results indicate that gibbsite was the RM phase more involved in the interaction with As(V) at the three pH values considered. The evidence was in agreement with the identification of the crystalline phases reported in Table 2, which showed the disappearance of gibbsite in As(V)-RM samples at pH 4.0, 7.0, and 10.0.

Thermal analyses of P(V)-RM samples at pH 4.0, 7.0, and 10.0. In the thermograms of P(V)-RM at pH 4.0 and 7.0, the weight loss in the range 200−400ºC, with a peak at 267ºC, disappeared (Figure 4). This could be attributed to the dissolution of cancrinite and sodalite phases at pH 7.0 and of sodalite at pH 4.0, following the interaction with phosphate anions, as indicated by the XRD analyses (Table 2). Besides, the DTG curves of P(V)-RM at pH 4.0 and 7.0 showed two distinct weight losses between 180 and 400ºC, with temperature peaks at 205ºC and 275ºC at pH 4.0 and at 230ºC and 275ºC at pH 7.0 (Figure 4). These weight losses could be ascribed to the elimination of crystallization water (adsorbed and/or coordinated) of metal-phosphate precipitates such as Fe phosphate (Scaccia *et al.*, 2002; 2003) and/or Al phosphate (Tanaka and Chikazawa, 2000; Chen *et al.*, 2003). The precipitates were probably derived from the reaction between phosphate and framework cations from the solubilization of RM phases more reactive towards this anion, *e.g.* gibbsite, hematite, and sodalite. The weight losses in the 180−400ºC range were 5.68% and 6.21% in thermograms of P(V)-RM at pH 4.0 and 7.0, respectively (Table 4).

A small weight loss between 480 and 600ºC, with a peak at 500ºC, in the thermograms of P(V)-RM at pH 4.0 and 7.0 of 2.88% and 1.73%, respectively, also occurred (Figure 4). The weight loss can be attributed both to the

glass transition of metal phosphates as suggested by Guo and Chen (1996) for Al phosphates, and to structural transformation of the metal-phosphate framework, according to the results of Scaccia *et al.* (2002), a study which investigated the thermal stability of Fe phosphate obtained by spontaneous precipitation from aqueous solutions. The results indicated that gibbsite, hematite, and sodalite were the RM phases more involved in the sequestration of phosphate mainly through co-precipitation reactions.

CONCLUSIONS

The results obtained showed that red muds (RM) are able to accumulate arsenate and phosphate ions through adsorption and precipitation reactions. The two anions showed a different reactivity toward the RM phases, the phosphate being sorbed more than the arsenate, because of the different mechanisms governing the sorption of these anions. Arsenate and phosphate sorption by RMs was accompanied by the formation of As(V)- or P(V)-Al amorphous precipitates as a consequence of gibbsite solubilization. In addition, only phosphate promoted the partial dissolution of hematite and the complete dissolution of sodalite, causing the formation of a new phosphatic phase, berlinite. This result is particularly significant and highlights the importance of precipitation reactions for phosphate fixation rather than the structural entrapment and exchange processes.

The results presented here suggest that gibbsite was the most active RM phase in the retention of As(V) and P(V) at all pH values examined. The very small gibbsite content in RM does not justify entirely the large degree of adsorption of As(V) and P(V) observed. Indeed, other RM phases such as hematite and sodalite were fundamental in the sequestration processes of As(V) and P(V).

The gibbsite solubilization following the reaction with As(V) and P(V) could have some negative environmental implications due to the release of Al, which may limit the use of RM as sorbing agents for polluted soils and waters. As phosphate is a common ion in soils and water, future studies are needed to evaluate the role of phosphate in the sorption processes of arsenate by RM when both are present together.

ACKNOWLEDGMENTS

REFERENCES

Antelo, J., Avena, M., Fiol, S., López, R., and Arce, F. (2005) Effects of pH and ionic strength on the adsorption of phosphate and arsenate at the goethite−water interface. *Journal of Colloid and Interface Science*, **285**, 476−486.

Budroni, G., Cocco, G., Jiang, J. Z., Carturan, G., and Enzo, S. (2000) X-ray powder diffraction and Moessbauer study of red mud residue from alumina production. *Materials Science Forum*, **343**, 2−7.

Castaldi, P., Silvetti, M., Santona, L., Enzo, S., and Melis, P. (2008) XRD, FT-IR, and thermal analysis of bauxite ore-processing waste (red mud) exchanged with heavy metals. *Clays and Clay Minerals*, **56**, 461−469.

Castaldi, P., Melis, P., Silvetti, M., Deiana, P., and Garau, G. (2009) Influence of pea and wheat growth on Pb, Cd, and Zn mobility and soil biological status in a polluted amended soil. *Geoderma*, **151**, 241−248.

Castaldi, P., Silvetti, M., Enzo, S., and Melis, P. (2010a) Study of sorption processes and FT-IR analysis of arsenate sorbed onto red muds (a bauxite ore processing waste). *Journal of Hazardous Materials*, 175, 172−178.

Castaldi, P., Silvetti, M., Garau, G., and Deiana, S. (2010b) Influence of the pH on the accumulation of phosphate by red mud (a bauxite ore processing waste). *Journal of Hazardous Materials*, **182**, 266−272.

Cengeloglu, Y., Tor, A., Arslan, G., Ersoz, M., and Gezgin, S. (2007) Removal of boron from aqueous solution by using neutralized red mud. *Journal of Hazardous Materials*, 142, 412−417.

Chen, D., He, L., and Shang, S. (2003) Study on aluminium phosphate binder and related Al_2O_3-SiC ceramic. *Materials Science and Engineering A − Structural Materials Properties Microstructure and Processing*, **348**, 29−35.

Ciardelli, M.C., Xu, H., and Sahai, N. (2008) Role of Fe(II), phosphate, silicate, sulfate, and carbonate in arsenic uptake by coprecipitation in synthetic and natural groundwater. *Water Research*, **42**, 615−624.

Garau, G., Castaldi, P., Santona, L., Deiana, P., and Melis, P. (2007) Influence of red mud, zeolite and lime on heavy metal immobilization, culturable heterotrophic microbial populations and enzyme activities in a contaminated soil. *Geoderma*, **142**, 47−57.

Garau, G., Silvetti, M., Deiana, S., Deiana, P., and Castaldi, P. (2011) Long term influence of red mud on As mobility and soil physico-chemical and microbial parameters in a polluted sub-acidic soil. *Journal of Hazardous Materials*, 185, 1241−1248.

Genç-Fuhrman, H., Bregnhoj, H., and McConchie, D. (2005) Arsenate removal from water using sand-red mud columns. *Water Research*, **13**, 2944−2954.

Goldberg, S. and Johnston, C.T. (2001) Mechanisms of arsenic adsorption on amorphous oxides evaluated using macroscopic measurements, vibrational spectroscopy, and surface complexation modeling. *Journal of Colloid and Interface Science*, **234**, 204−216.

Gray, C.W., Dunham, S.J., Dennis, P.G., Zhao, F.J., and McGrath, S.P. (2006) Field evaluation of in situ remediation of a heavy metal contaminated soil using lime and red-mud. *Environmental Pollution*, **142**, 530−539.

Guo, G. and Chen, Y. (1996) Thermal analysis and infrared measurements of a lead-barium-aluminium phosphate glass. *Journal of Non-Crystalline Solids*, **201**, 262−66.

Huang, W., Wang, S., Zhu, Z., Li, L., Yao, X., Rudolph, V., and Haghseresht, F. (2008) Phosphate removal from wastewater using red mud. *Journal of Hazardous Materials*, **158**, 35−42.

Linares, C.F., Sánchez, S., Urbina de Navarro, C., Rodríguez, K., and Goldwasser, M.R. (2005) Study of cancrinite-type zeolites as possible antiacid agents. *Microporous and Mesoporous Materials*, **77**, 215−221.

Liu, Y., Lin, C., and Wu, Y. (2007) Characterization of red mud derived from a combined Bayer. Process and bauxite calcination method. *Journal of Hazardous Materials*, **146**, 255−261.

Lombi, E., Hamon, R.E., Wieshammer, G., McLaughlin, M.J., and McGrath, S.P. (2004) Assessment of the use of industrial by-products to remediate a copper- and arsenic-

contaminated soil. *Journal of Environmental Quality*, **33**, 902−910.

Luengo, C., Brigante, M., and Avena, M. (2007) Adsorption kinetics of phosphate and arsenate on goethite. A comparative study. *Journal of Colloid and Interface Science*, **311**, 354−360.

Luxton, T.P., Eick, M.J., Rimstidt, D.J. (2008) The role of silicate in the adsorption/desorption of arsenite on goethite. *Chemical Geology*, **252**, 125−135.

Manning, B.A. and Goldberg, S. (1996) Modeling competitive adsorption of arsenate with phosphate and molybdate on oxide sminerals. *Soil Science Society of America Journal*, **60**, 121−131.

Mon, J., Deng, Y., Flury, M., and Harsh, J.B. (2005) Cesium incorporation and diffusion in cancrinite, sodalite, zeolite and allophone. *Microporous and Mesoporous Materials*, **86**, 277−286.

Palmer, S.J., Soisonard, A., and Frost, R.L. (2009) Determination of the mechanism(s) for the inclusion of arsenate, vanadate, or molybdate anions into hydrotalcites with variable cationic ratio. *Journal of Colloid and Interface Science*, **329**, 404−409.

Pontikes, Y., Nikolopoulos, P., and Angelopoulos, G.N. (2007) Thermal behaviour of clay mixtures with bauxite residue for the production of heavy-clay ceramics. *Journal of the European Ceramic Society*, **27**, 1645−1649.

Pradhan, J., Das, S.N., and Thakur, R.S. (1999) Adsorption of exavalent chromium from aqueous solution by using activated red mud. *Journal of Colloid and Interface Science*, **217**, 137−141.

Rojsajjakul, T., Veravong, S., Tumcharern, G., Seangprasertkij-Magee, R., and Tuntulani, T. (1997) Synthesis and characterisation of polyaza crown ether derivatives of calix arene and their role as anion receptors. *Tetrahedron*, **53**, 4669−4680.

Ruixia, L., Jinlong, G., and Hongxiao, T. (2002) Adsorption of fluoride, phosphate, and arsenate ions on a new type of ion exchange fiber. *Journal of Colloid and Interface Science*, **248**, 268−274.

Scaccia, S., Carewska, M., Di Bartolomeo, A., and Prosini, P.P. (2002) Thermoanalytical investigation of iron phosphate obtained by spontaneous precipitation from aqueous solutions. *Thermochimica Acta*, **383**, 145−152.

Scaccia, S., Carewska, M., Di Bartolomeo, A., and Prosini, P.P. (2003) Thermoanalytical investigation of nanocrystal-line iron(II) phosphate obtain by spontaneous precipitation from aqueous solutions. *Thermochimica Acta*, **397**, 135−41.

Sglavo, V.M., Campostrini, R., Maurina, S., Carturan, G., Monagheddu, M., Budroni, G., and Cocco, G. (2000) Bauxite red mud in the ceramic industry. Part 1: thermal behaviour. *Journal of the European Ceramic Society*, **20**, 235−244.

Smiljanić, S., Smičiklas, I., Perić-Grujić, A., Lončar, B., and Mitrić, M. (2010) Rinsed and thermally treated red mud sorbents for aqueous Ni^{2+} ions. *Chemical Engineering Journal*, **162**, 75−83.

Tanaka, H. and Chikazawa, M. (2000) Modification of amorphous aluminum phosphate with alkyl phosphates. *Materials Research Bulletin*, **35**, 75−84.

Tor, A., Danaoglu, N., Arslan, G., and Cengeloglu, Y. (2009) Removal of fluoride from water by using granular red mud: batch and column studies. *Journal of Hazardous Materials*, **164**, 271−278.

Violante, A., Pucci, M., Cozzolino, V., Zhu, J., and Pigna, M. (2009) Sorption/desorption of arsenate on/from Mg−Al layered double hydroxides: Influence of phosphate. *Journal of Colloid and Interface Science*, **333**, 63−70.

Wang, S. and Mulligan, C.N. (2008) Speciation and surface structure of inorganic arsenic in solid phases: A review. *Environment International*, **34**, 867−879.

Wang, S., Ang, H.M., and Tad, M.O. (2008) Novel applications of red mud as coagulant, adsorbent and catalyst for environmentally benign processes. *Chemosphere*, **72**, 1621−1635.

Young, R.A. (1993) *The Rietveld Method*. Oxford University Press, Oxford, UK.

Zhang, H. and Selim, H.M. (2008) Competitive sorption-desorption kinetics of arsenate and phosphate in soils. *Soil Science*, **173**, 3−12.

Zhang, S., Liu, C., Luan, Z., Peng, X., Ren, H., and Wang, J. (2008) Arsenate removal from aqueous solutions using modified red mud. *Journal of Hazardous Materials*, **152**, 486−492.

Zhao, Y., Wang, J., Luan, Z., Peng, X., Liang, Z., and Shi, L. (2009) Removal of phosphate from aqueous solution by red mud using a factorial design. *Journal of Hazardous Materials*, **165**, 1193−1199.